iScience

CellPress
OPEN ACCESS

Article

Role of SPTSSB-Regulated de Novo Sphingolipid Synthesis in Prostate Cancer Depends on Androgen Receptor Signaling

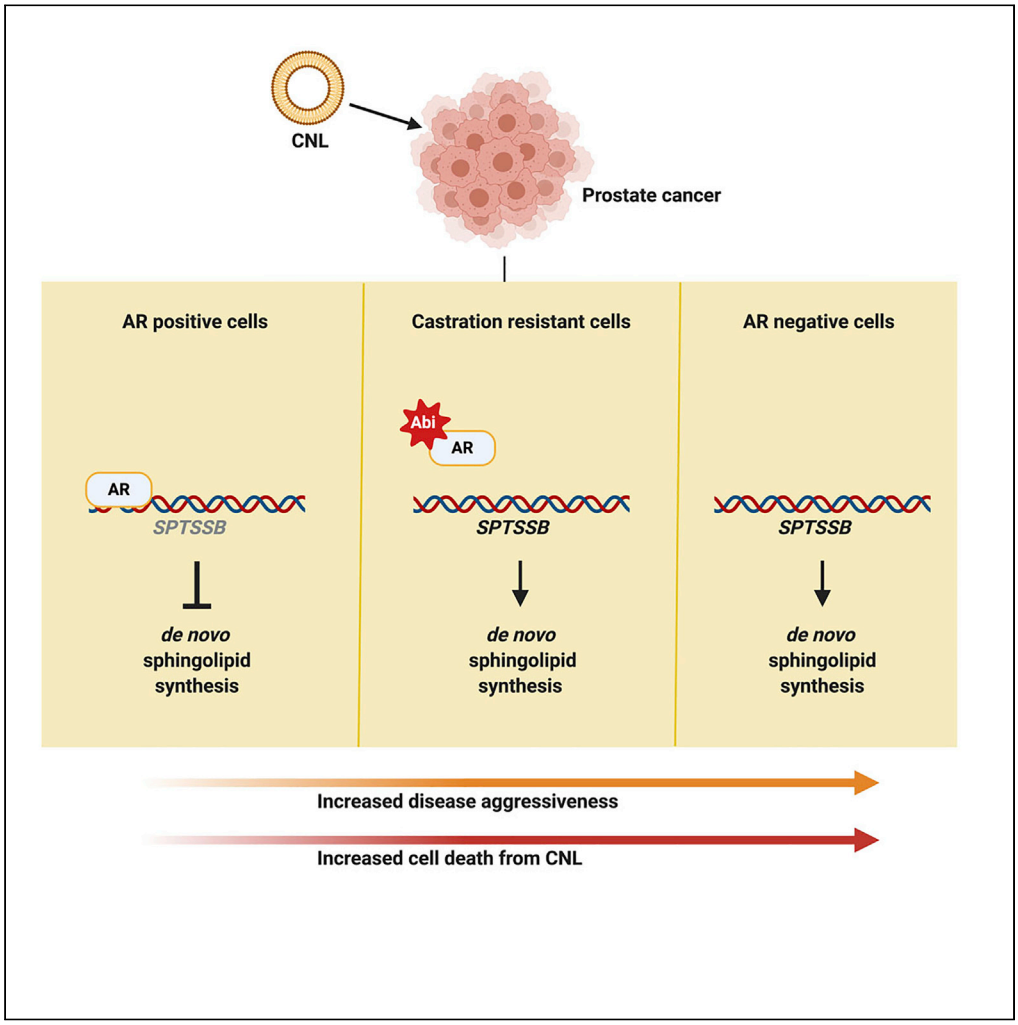

Pedro Costa-Pinheiro, Abigail Heher, Michael H. Raymond, ..., Susan J. Walker, Todd E. Fox, Mark Kester

mk5vq@virginia.edu

HIGHLIGHTS

AR-negative PCa cells are more susceptible to CNL than AR-positive cells

Combination of anti-androgens and CNL results in enhanced efficacy for AR-positive PCa

AR negatively regulates the *de novo* synthesis of sphingolipids through SPTSSB

SPTSSB is crucial for CNL effect in AR-negative PCa and is upregulated in neuroendocrine tumors

Costa-Pinheiro et al., iScience *23*, 101855
December 18, 2020
https://doi.org/10.1016/j.isci.2020.101855

iScience

CellPress
OPEN ACCESS

Article

Role of SPTSSB-Regulated de Novo Sphingolipid Synthesis in Prostate Cancer Depends on Androgen Receptor Signaling

Pedro Costa-Pinheiro,[1] Abigail Heher,[2] Michael H. Raymond,[3] Kasey Jividen,[4] Jeremy JP. Shaw,[1] Bryce M. Paschal,[4,5] Susan J. Walker,[6] Todd E. Fox,[6] and Mark Kester[6,7,8,*]

SUMMARY

Anti-androgens are a common therapy in prostate cancer (PCa) targeting androgen receptor (AR) signaling. However, these therapies fail due to selection of highly aggressive AR-negative cancer cells that have no therapeutic options available. We demonstrate that elevating endogenous ceramide levels with administration of exogenous ceramide nanoliposomes (CNLs) was efficacious in AR-negative cell lines with limited efficacy in AR-positive cells. This effect is mediated through reduced *de novo* sphingolipid synthesis in AR-positive cells. We show that anti-androgens elevate *de novo* generation of sphingolipids via *SPTSSB*, a rate-limiting mediator of sphingolipid generation. Moreover, pharmacological inhibition of AR increases the efficacy of CNL in AR-positive cells through *de novo* synthesis, while SPTSSB knockdown limited CNL's efficacy in AR-negative cells. Alluding to clinical relevance, SPTSSB is upregulated in patients with advanced PCa after anti-androgens treatment. These findings emphasize the relevance of AR regulation upon sphingolipid metabolism and the potential of CNL as a PCa therapeutic.

INTRODUCTION

Prostate cancer (PCa) is the most incident cancer in the United States male population, responsible for 20% of newly diagnosed cases (Siegel et al., 2020). Moreover, PCa is estimated to account for 10% of cancer-related deaths in the male population and has the second highest mortality rate (Siegel et al., 2020). Effective treatment of PCa remains elusive due to disease heterogeneity and complex disease progression (Shen and Abate-Shen, 2010). Androgens are necessary for normal development and functional maintenance of healthy prostatic tissue but also contribute to PCa onset and progression (Narayanan et al., 2016). Androgens are natural ligands of androgen receptor (AR), a transcription factor that regulates several key cellular pathways such as proliferation and lipid metabolism (Mills, 2014). Pharmacological inhibition of androgen synthesis or the receptor are currently the main therapeutic approaches for patients with advanced PCa (Damber and Aus, 2008). Despite symptom relief, virtually all patients develop recurrence within 24 months by progression to castration-resistant prostate cancer (CRPCa) (Felici et al., 2012; Nadiminty et al., 2013). Mechanisms of resistance to AR-signaling inhibitors in CRPCa patients include restored AR activity, hypersensitivity to androgens, and ligand-independent AR activation (Ramon and Denis, 2007; Zong and Goldstein, 2013). An alternative mechanism of resistance involves cell transdifferentiation to AR-negative neuroendocrine phenotype (CRPCa-NE) after androgen deprivation therapy (ADT) (Ramon and Denis, 2007; Zong and Goldstein, 2013; Zou et al., 2017). The emergence of this phenotype has been associated with worse prognosis and has features of both small-cell carcinoma and neuroendocrine differentiation (Aggarwal et al., 2014). Most PCa-related deaths occur due to CRPCa, which lacks any efficacious treatments (Damber and Aus, 2008). Therefore, it is imperative to understand the mechanisms of resistance and develop new therapeutic modalities for patients with CRPCa.

Cytotoxic agents, including AR-signaling inhibitors, and radiation therapy, have been shown to lead to an accumulation of sphingolipids, including pro-death ceramides (Kolesnick and Fuks, 2003; Modrak et al., 2006; Murdica et al., 2018; Ogretmen, 2018). Sphingolipids are bioactive lipids that have not only a structural role in organelle and plasma membranes but also regulate signaling pathways (Hannun and Obeid, 2018; Maceyka and Spiegel, 2014). Dysregulation of sphingolipid metabolic enzymes is associated with

[1]Department of Pathology, University of Virginia, Charlottesville, VA 22903, USA

[2]Department of Biology, University of Virginia, Charlottesville, VA 22903, USA

[3]Neuroscience Graduate Program, University of Virginia, Charlottesville, VA 22903, USA

[4]Center for Cell Signaling, University of Virginia, Charlottesville, VA 22903, USA

[5]Department of Biochemistry and Molecular Genetics, University of Virginia, Charlottesville, VA 22903, USA

[6]Department of Pharmacology, University of Virginia, Charlottesville, VA 22903, USA

[7]nanoSTAR Institute, University of Virginia, Charlottesville, VA 22903, USA

[8]Lead contact

*Correspondence: mk5vq@virginia.edu

https://doi.org/10.1016/j.isci.2020.101855

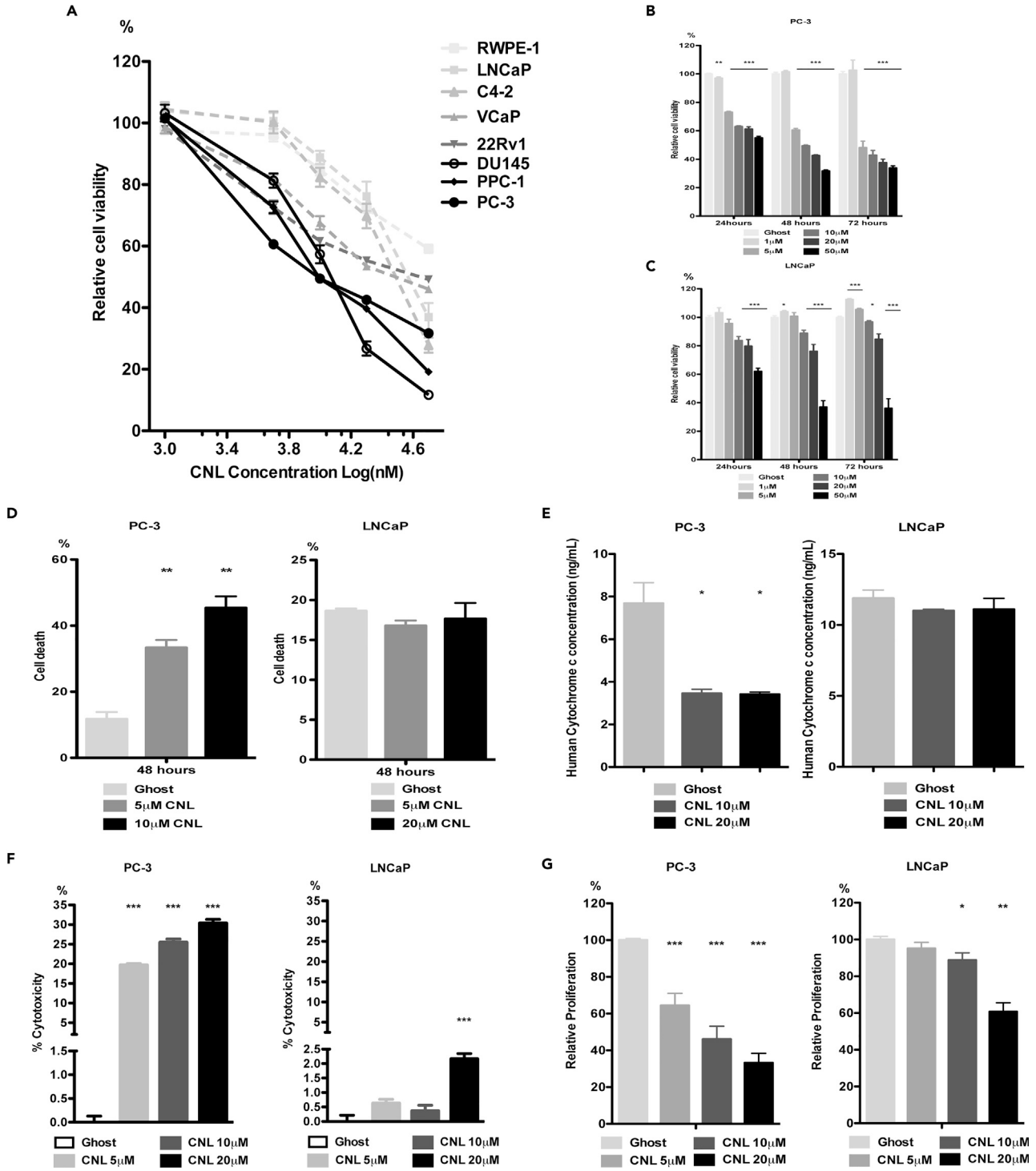

Figure 1. CNL are Efficacious against Highly Aggressive AR-Negative PCa Cells

(A) Viability of 7 PCa cell lines and 1 normal prostate epithelial cell line (RWPE-1) after 48hr of CNL treatment (1, 5, 10, 20, 50μM) compared to ghost control (20μM). Mean ± SEM from three independent experiments is represented. Gray – AR-positive cell lines; Black – AR-negative cell lines.

(B and C) Effect of time and concentration of CNL on the viability of (B) AR-negative cell line (PC-3) and (C) AR-positive cell line (LNCaP) compared to ghost control. Mean ± SEM from three independent experiments is represented. *p* values obtained using non-parametric Mann–Whitney *U*-test: *, **, and *** represent significance of p values < 0.05, 0.01, and 0.001 respectively.

Figure 1. *Continued*

(D) Cell death measured after 48hr of ghost and CNL treatment in PC-3 and LNCaP. Mean ± SEM from three independent experiments is represented. *p* values obtained using non-parametric Mann–Whitney *U*-test: ** represent significance of p values < 0.01.

(E) Mitochondria cytochrome *c* in PC-3 and LNCaP cells treated with CNL and ghost control for 48hr. Mean ± SEM from three independent experiments is represented. p values obtained using a two-tailed *t* test: * represent significance of p values < 0.05.

(F) Cytotoxicity of CNL treatments in PC-3 and LNCaP after 48hr compared to ghost control. Mean ± SEM from three independent experiments is represented. *p* values obtained using non-parametric Mann–Whitney *U*-test: *** represent significance of p values < 0.001.

(G) Cell proliferation measured in PC-3 and LNCaP cells treated with CNL and ghost control for 48hr. Mean ± SEM from three independent experiments is represented. *p* values obtained using non-parametric Mann–Whitney *U*-test: *, **, and *** represent significance of p values < 0.05, 0.01, and 0.001, respectively.

cancer progression (Beckham et al., 2012; McNair et al., 2017; Ryland et al., 2011; Saad et al., 2007; Voelkel-Johnson et al., 2018). Moreover, ceramide accumulation in tumors is associated with cancer cell death, which emphasizes the potential role of ceramide as a cancer treatment (Grosch et al., 2012; Hannun and Obeid, 2018; Maceyka and Spiegel, 2014; Ogretmen, 2018; Shaw et al., 2018; Taha et al., 2006). *De novo* synthesis of ceramide and other sphingolipids is achieved by condensation of L-serine with an acyl-CoA substrate (Davis et al., 2018). In mammals, several enzymes are involved in this process: three serine palmitoyltransferase long-chain (SPTLC1-3) subunits, two serine palmitoyltransferase small subunits (SPTSSA-B), and three ORMDL sphingolipid biosynthesis regulator (ORMDL1-3) (Han et al., 2009). The formation of a complex between 2 SPTLCs and SPTSSA or SPTSSB leads to the generation of dihydrosphingosine, a precursor sphingolipid that can result in accumulation of ceramide. Dihydrosphingosine is a bioactive lipid that influences cell signaling and has been associated with neurodegeneration (Zhao et al., 2015). These enzymes maintain tight control over the generation of ceramides, as sphingolipid accumulation can lead to several disruptions in cells and to various pathologies (Di Pardo et al., 2017; Dolgachev et al., 2004; Ogretmen, 2018). Not only do sphingolipids have a role in predicting patient outcomes in PCa, the sphingolipid profile also undergoes remodeling in response to conventional PCa treatments (Lin et al., 2017; Murdica et al., 2018). However, the underlying mechanisms and consequences of altered sphingolipid metabolism in PCa remain unclear.

Our laboratory has developed a non-toxic and biologically stable nanoliposome formulation that includes C6-ceramide nanoliposomes (CNLs), as a potential cancer therapeutic. CNL demonstrates selectivity for tumor cells in preclinical models and also exhibits minimal toxicity in an ongoing phase I clinical trial (NCT number NCT02834611) (Barth et al., 2011; Kester et al., 2015). In the present work, we have discovered that CNL efficacy is determined by AR signaling in PCa. Through these findings, we determined that CNL treatment is more effective in highly aggressive AR-negative disease models. This efficacy occurs through elevation of SPTSSB-dependent *de novo* synthesis of ceramide, an understudied pathway in PCa cancer.

RESULTS

CNL Is More Efficacious against AR-Negative Than AR-Positive PCa Cells

To determine the efficacy of C6-CNL in PCa, 7 PCa cell lines and a normal prostate epithelial cell line (RWPE-1) were utilized. These cells were treated with various concentrations of CNL for 72 hr, and viability was determined relative to ghost nanoliposomes, the vehicle control that contains no bioactive C6-ceramide (Figure 1A, Figure S1A–S1F). Notably, cells that don't express AR, representative of most aggressive tumors, were the most sensitive to CNL (Figure 1B). Given the observed dichotomy in the response to CNL depending on AR status, we selected two of the most widely studied preclinical models representative cell lines of PCa: PC-3 (AR-negative) and LNCaP (AR-positive) for further studies. We treated PC-3 and LNCaP cells with various concentrations of CNL across three different timepoints, and observed that the efficacy of CNL was more efficacious in PC-3 cells in a time- and concentration-dependent manner (Figures 1B and 1C). These data demonstrate that CNL is most effective in the most aggressive form of CRPCa represented by lack of AR.

To further confirm our viability results, we measured the effect of CNL on different phenotypic readouts in the same cell lines. CNL increased cell death in AR-negative PC-3 cells compared with the control group, while cell death was not altered in AR-positive LNCaP cells (Figure 1D). Increase in cell death in PC-3 cells was observed to be concentration-dependent at 24 hr (Videos S1, S2, S3, and S4). CNL treatment in AR-negative cells also reduced mitochondrial cytochrome *c* levels, while these were unchanged in AR-positive cells (Figure 1E). Additionally, CNL induced greater release of lactate dehydrogenase in AR-negative cells than in AR-positive cells showing differential toxicity in these cells (Figure 1F). Similarly, CNL reduced

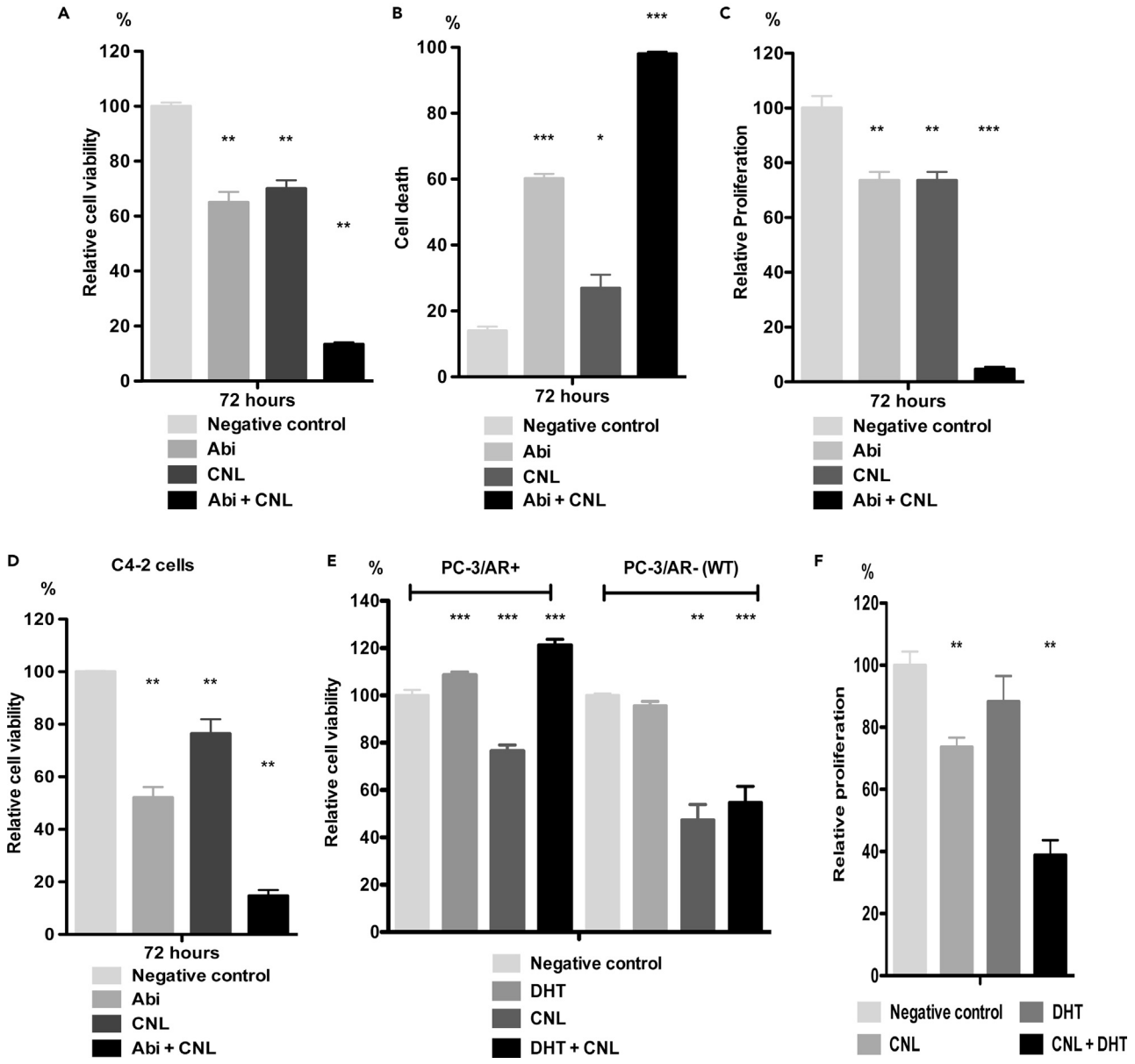

Figure 2. Intact AR Signaling Hinders CNL Efficacy in PCa Cells

(A) Viability of LNCaP cells measured after 72hr of treatment with Abi (20μM), CNL (20μM), or combo (20μM + 20μM) compared to negative control (EtOH + ghost). Mean ± SEM from three independent experiments is represented. *p* values obtained using non-parametric Mann–Whitney *U*-test: ** represent significance of p values < 0.01.

(B) Cell death of LNCaP cells after 72hr of treatment with Negative control (EtOH + ghost), Abi (20μM), CNL (20μM), or Combo (20μM + 20μM). Mean ± SEM from three independent experiments is represented. *p* values obtained using non-parametric Mann–Whitney *U*-test: * and *** represent significance of p values < 0.05 and 0.001, respectively.

(C) Proliferation of LNCaP cells treated with Abi (20μM), CNL (20μM), or Combo (20μM + 20μM) for 72hr and compared to Negative control. Mean ± SEM from three independent experiments is represented. *p* values obtained using non-parametric Mann–Whitney *U*-test: ** and *** represent significance of p values < 0.01 and 0.001, respectively.

(D) Viability of C4-2 cells measured after 72hr of treatment with Abi (20μM), CNL (20μM), or Combo (20μM + 20μM) compared to Negative control (EtOH + ghost). Mean ± SEM from three independent experiments is represented. *p* values obtained using non-parametric Mann–Whitney *U*-test: ** represent significance of p values < 0.01.

(E) Viability of PC-3/AR+ and PC-3/WT cells after 24hr of DHT (1nM) pretreatment followed by 48hr of CNL (10μM) compared to negative control (EtOH + ghost). Mean ± SEM from three independent experiments is represented. *p* values obtained using non-parametric Mann–Whitney *U*-test: ** and *** represent significance of p values < 0.01 and 0.001, respectively.

Figure 2. *Continued*
(F) Proliferation of LNCaP cells treated with dihydrotestosterone (100nM) for 24hr followed by CNL (20μM) or ghost for 48hr and compared to negative controls. Mean ± SEM from three independent experiments is represented. *p* values obtained using non-parametric Mann–Whitney *U*-test: ** represent significance of p values < 0.01.

proliferation in PC-3 cells when compared with LNCaP cells (Figure 1G). Taken together, these results suggest the importance of AR status in affecting the efficacy of CNL in PCa cells and the potential of CNL for the most aggressive neuroendocrine advanced PCa.

CNL Efficacy Is Enhanced in the Presence of Anti-androgens

Given the reduced efficacy of CNL in AR-positive cells, we sought to determine if inhibiting AR signaling would enhance the effect of CNL as to mimic the effect observed in AR-negative cell lines. We combined CNL and abiraterone acetate (Abi), an FDA-approved drug that suppresses production of androgens and is a partial AR antagonist (Richards et al., 2012). We showed that combining Abi with CNL had an enhanced effect on reducing LNCaP cell viability (Figure 2A) and increased cell death (Figure 2B). The same phenomenon was observed when measuring cell proliferation, as combining both drugs significantly reduced cell proliferation (Figure 2C). The inhibitory effect of Abi on AR signaling was confirmed, as demonstrated by significant reductions of two downstream targets of AR, PSA (*KLK3*), and *FKPB5* (Figure S2A). We next tested C4-2 cells that are representative of AR-indifference tumors, which do not rely on androgens for growth but are still positive for AR signaling. We observed the same response pattern as in LNCaP cells (Figure 2A), where the combination of Abi and CNL led to enhanced reduction in cell viability of C4-2 cells (Figure 2D). Finally, we expanded our work to another FDA-approved drug for PCa: enzalutamide (MDV3100), an AR antagonist. Validating the Abi results, the effect of MDV3100 and CNL was augmented by the combination of both drugs (Figures S2B–S2D). These data show that combining AR inhibitors with CNL facilitated cell death in AR-positive PCa cells.

AR Signaling Impairs the Response to CNL Treatment

To further test the importance of AR signaling in the response to CNL, we used PC-3 cells genetically engineered to express AR (PC-3/AR+) to determine if re-introduction of AR would decrease CNL efficacy. Under androgen-deficient conditions, we found no difference between PC-3/WT and PC-3/AR+ in the response to CNL (data not shown). However, when we tested the effect of CNL on PC-3/AR + cells in the presence of dihydrotestosterone (DHT) to stimulate androgen signaling, we found that PC-3/AR + exhibited diminished efficacy toward CNL treatment (Figure 2E). These data suggest that activation of AR signaling is sufficient to impair CNL treatment in PCa cells.

In PCa cell lines, AR signaling is rapidly induced by androgen stimulation. However, due to a biphasic growth phenomenon, high doses of androgens can prevent AR-induced cell growth (de Launoit et al., 1991; Lee et al., 1995; Tsihlias et al., 2000). We confirmed these findings by showing that low concentrations of DHT (1nM and 10nM) significantly increased cell proliferation relative to vehicle control, in contrast to high dose of DHT (100nM and 1μM) where proliferation remained either unchanged or significantly decreased (Figure S2E). To further investigate the hypothesis that AR signaling facilitates resistance to CNL, we abrogated AR signaling with high androgen dosages followed by CNL treatment in AR-positive cells. The combination of CNL and blocking AR-driven cell growth with high dose DHT resulted in significantly lower rates of cellular proliferation (Figures 2F and S2F). These data further support the idea that AR signaling impairs the efficacy of CNL in PCa cells.

Inhibition of AR Signaling with Abiraterone Acetate Increases *De Novo* Synthesis of Sphingolipids

Given the enhanced effect of combining Abi and CNL in AR-positive cells, we sought to determine the impact of combining both drugs on sphingolipid metabolism. Mammalian cells have the ability to convert exogenous ceramides to natural occurring sphingolipids, adding importance to studies of sphingolipid metabolism after CNL treatment. C6-ceramide levels were measured to determine equivalent uptake between different treatment groups as well as metabolic conversion to endogenous ceramides after treatment. Interestingly, we observed that Abi led to more sustained levels of C6-ceramide compared to CNL treatment alone (Figure 3A). We also found the total mass of endogenous ceramides was significantly increased in the presence of both drugs (Figure 3B) relative to the negative control. Moreover, we report for the first time a significant increase in dihydrosphingosine in AR-positive cells

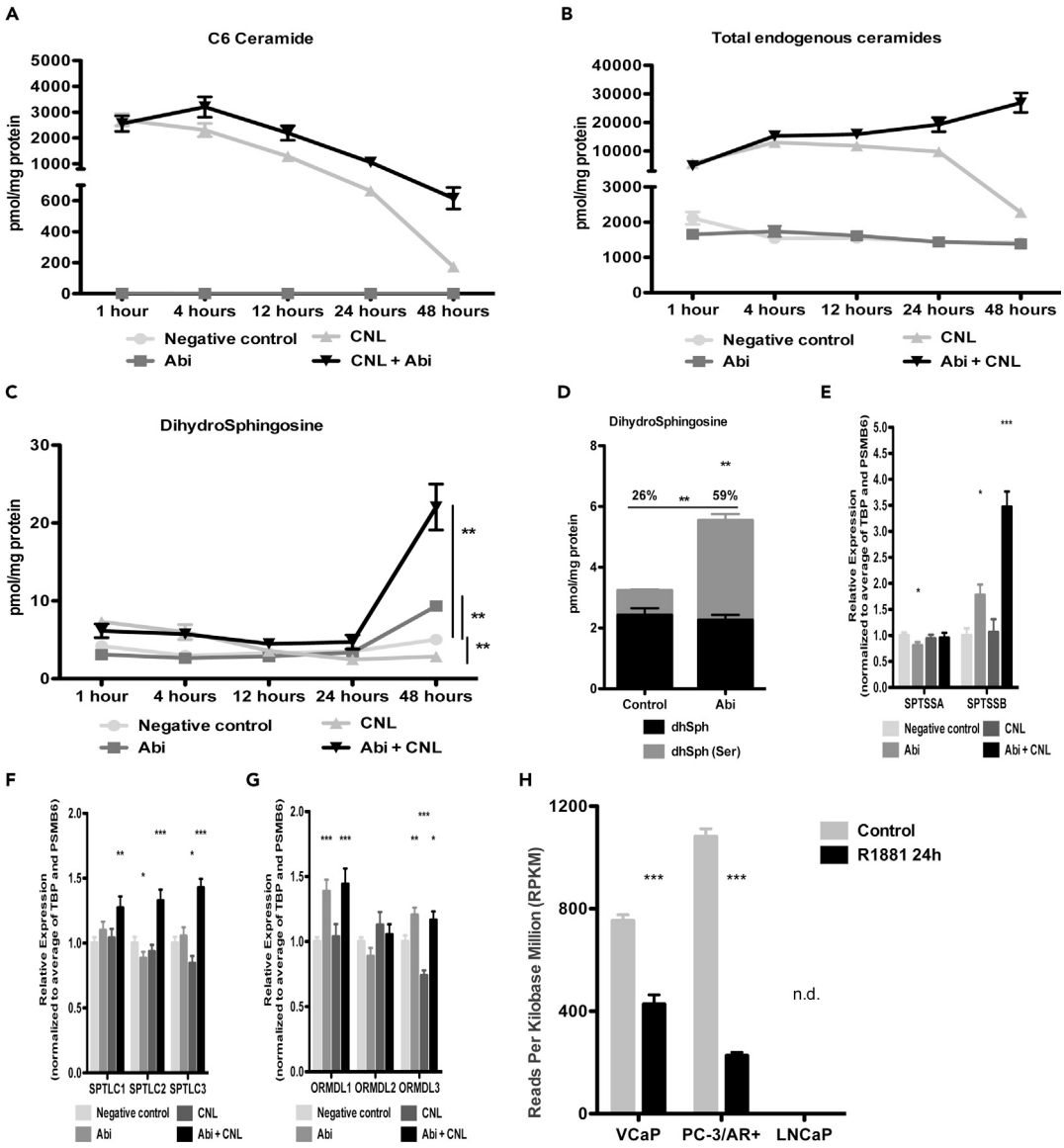

Figure 3. *De novo* Synthesis of Sphingolipids is Negatively Regulated by AR

(A–C) Mass of (A) C6-ceramide, (B) Total endogenous ceramides, (C) Dihydrosphingosine in LNCaP cells treated with Negative control (EtOH + ghost), Abi (10μM), CNL (10μM), or Combo (10μM + 10μM). Mean ± SEM (n = 5) is represented.

(D) Mass of dihydrosphingosine d18:1 in LNCaP cells pulsed with L-Serine-13C3 for 2h followed by treatment with Negative control (EtOH) or Abi (10μM) for 48hr. Mean ± SEM (n = 5) is represented. *p* values obtained using non-parametric Mann–Whitney *U*-test: ** represent significance of p values < 0.01.

(E–G) Gene expression of (E) *SPTSSA* and *SPTSSB*; (F) *SPTLC1, SPTLC2,* and *SPTLC3*; (G) *ORMDL1, ORMDL2,* and *ORMDL3* in LNCaP cells treated with Abi (10μM), CNL (10μM), or Combo (10μM + 10μM) for 48hr compared to Negative control (EtOH + ghost). Mean ± SEM from three independent experiments is represented. *p* values obtained using non-parametric Mann–Whitney *U*-test: *, **, and *** represent significance of p values < 0.05, 0.01, and 0.001 respectively.

(H) *SPTSSB* expression from RNA-seq in VCaP, PC-3/AR+, and LNCaP after AR stimulation with R1881 (1nM) for 24hr. Mean ± SEM from three independent experiments is represented. *p* values obtained using two-tailed *t* test: *** represent significance of p values < 0.001 respectively.

caused by Abi (Figure 3C), which was then augmented in the presence of CNL with Abi (Figure 3C). Importantly, dihydrosphingosine is a precursor of endogenous ceramides and is mostly generated by activation of *de novo* synthesis of sphingolipids. The accumulation of endogenous and exogenous ceramides, as well as dihydrosphingosine, in the presence of Abi and CNL is likely associated with enhanced cell death in LNCaP cells. These findings also suggested that AR signaling might negatively regulate *de novo* synthesis of sphingolipids.

To validate and trace augmented *de novo* sphingolipid synthesis, in the presence of anti-androgen, Abi, we implemented a novel mass spectrometry strategy. This technique requires the addition of isotope-labeled serine, a necessary amino acid for sphingolipid synthesis, to the cell culture growth media prior to anti-androgen treatment, thus enabling us to determine newly synthesized sphingolipid molecules. As expected, we observed a significant increase in dihydrosphingosine after Abi treatment in LNCaP cells and that this increase in dihydrosphingosine comes from newly synthesized lipids via the *de novo* synthesis pathway (Figure 3D). These data support our hypothesis that blocking AR signaling leads to increased *de novo* synthesis of sphingolipids.

Anti-Androgen Abiraterone Acetate Increases the Expression of Enzyme Regulators of *De Novo* Sphingolipid Synthesis

Given that AR can regulate transcription of thousands of gene transcripts in different cell pathways, we measured the mRNA expression of 8 enzymes involved in the initiation of *de novo* synthesis of sphingolipids after Abi treatment, with or without CNL, in AR-positive LNCaP cells. We observed that after 48 hr, 6 of the 8 enzymes (*ORMDL1, ORMDL3, SPTLC1, SPTLC2, SPTLC3*, and *SPTSSB*) tested had elevated expression levels after combination treatment, while two (ORMDL2 and SPTSSA) did not (Figures 3E–3G). Notably, Abi treatment increased the expression of SPTSSB by nearly 2-fold, which was then significantly augmented by CNL to nearly 3.5-fold, despite a lack of increase from CNL alone (Figure 3E). These data show that in AR-positive cells, the combination of Abi and CNL elevates expression of enzymes involved in the *de novo* synthesis of sphingolipids, consistent with the increased mass of dihydrosphingosine (Figure 3C).

To confirm regulation of SPTSSB by AR signaling, we analyzed an RNA sequencing data set of three different PCa cell lines stimulated for 24 hr with R1881, an AR agonist. The expression of *SPTSSB* was not detected in LNCaP in this experiment. However, in two other AR-positive cell lines (PC-3/AR+, VCaP) *SPTSSB* expression was significantly decreased after AR stimulation (Figure 3H). These data also support AR signaling negatively regulating *de novo* sphingolipid synthesis through SPTSSB.

CNL Increases de Novo Synthesis of Sphingolipids and Accumulation of Ceramides in AR-Negative Cells

To validate the importance of *de novo* sphingolipid synthesis driven by anti-androgens in in AR-positive cells, we sought to recapitulate these findings in AR-negative cells (PC-3) treated with CNL. After an initial increase in C6-ceramide following CNL addition, C6-ceramide levels decreased over time. However, after 48hr of CNL treatment, C6-ceramide levels remained considerably high (Figure 4A). More importantly, the total endogenous ceramide mass, which excludes exogenous C6-ceramide, increased in CNL-treated PC-3 cells compared to control cells (Figure 4B). Concomitant with this increase in total ceramide levels, we observed a significant increase in the *de novo* precursor dihydrosphingosine that peaked at 48hr (Figure 4C). This similar regulation of *de novo* synthesis of sphingolipids in AR-negative and AR-positive cells treated with Abi (Figure 3) support the notion that AR signaling can regulate CNL metabolism and ultimately determines CNL treatment response.

We then evaluated the impact of CNL treatment on the expression of de novo metabolic enzymes in PC-3 cells. We observed an overall increase in expression of the vast majority of these enzymes, which corroborates the increase in dihydrosphingosine mass observed in Figure 4C (Figure 4D). Of particular interest, expression of *SPTSSB* was elevated in PC-3 cells after CNL treatment similarly to the combination between Abi and CNL in AR-positive cells (Figure 3E). In LNCaP, CNL treatment alone for 24 hr did not alter the expression of these proteins except for a modest increase of *SPTLC2* expression (Figure 4E). Overall, the findings in Figures 3 and 4 support the hypothesis that CNL treatment increases *de novo* synthesis of sphingolipids only in the absence of AR signaling.

SPTSSB Expression Is Upregulated in Patients with Advanced PCa

To determine the clinical relevance of our findings regarding SPTSSB, we evaluated its expression across available TCGA PCa patient data sets. Using a paired analysis of tumor versus normal tissue, we determined that the expression of SPTSSB was significantly downregulated in tumors (Figure 5A) (Cerami et al., 2012). The comparison of all tumor samples versus the group of available normal samples also showed a reduction of *SPTSSB* expression in PCa (Figure 5B). Importantly, the expression analysis showed higher expression in samples with higher Gleason score, which represent more aggressive tumors

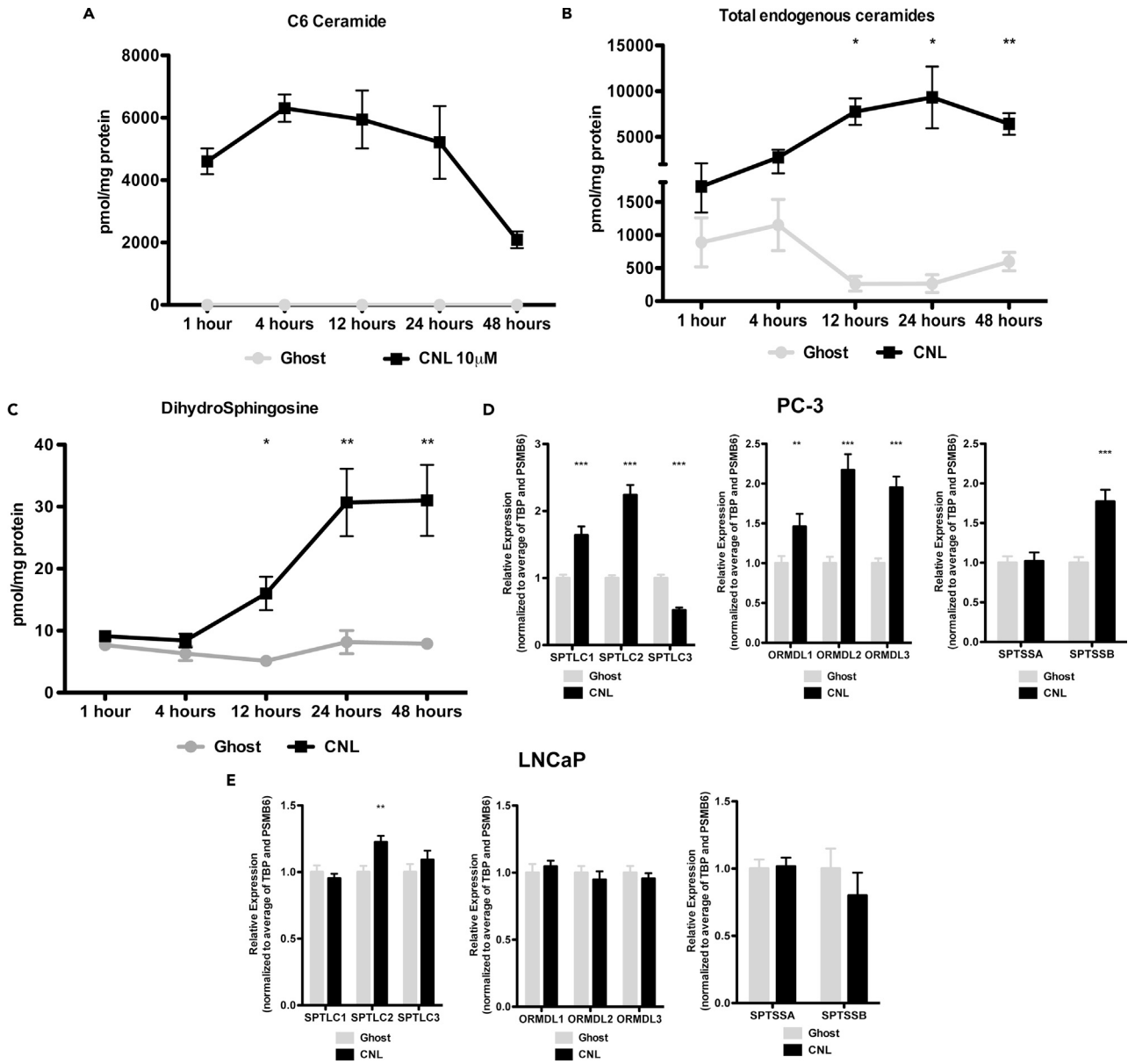

Figure 4. CNL Induces *de novo* Synthesis of Sphingolipids in AR-Negative Cells

(A–C) Mass of (A) C6-ceramide, (B) total endogenous ceramides, (C) dihydrosphingosine in PC-3 cells treated with ghost or CNL (10μM). Mean ± SEM (n = 5) is represented. *p* values obtained using non-parametric Mann–Whitney *U*-test: *, and ** represent significance of p values < 0.05 and 0.01, respectively. (D and E) Gene expression of SPTLC1-3, ORMDL1-3, SPTSSA, and SPTSSB in (D) PC-3 and (E) LNCaP cells after 24hr of CNL (10μM) treatment compared to ghost control. Mean ± SEM from three independent experiments is represented. *p* values obtained using non-parametric Mann–Whitney *U*-test: *, **, and *** represent significance of p values < 0.05, 0.01, and 0.001, respectively.

(Figure 5C). Interestingly, in the TCGA original data set, patients' AR score was negatively correlated with SPTSSB expression (Figure 5D, Spearman correlation: −0.24; $p < 0.001$) (Li et al., 2018).

Surveying *SPTSSB* expression in advanced cases of PCa also provides evidence that SPTSSB plays an important role in PCa. In a neuroendocrine CRPCa data set, we calculated that 28% of the patients had *SPTSSB* gene amplifications or increased mRNA levels (Figure 5E) (Beltran et al., 2016). A study from Fred Hutchinson Cancer Research Center that measured mRNA levels of genes from patients with disseminated PCa showed *SPTSSB* expression alterations, primarily increases, in 33% of patients that had received

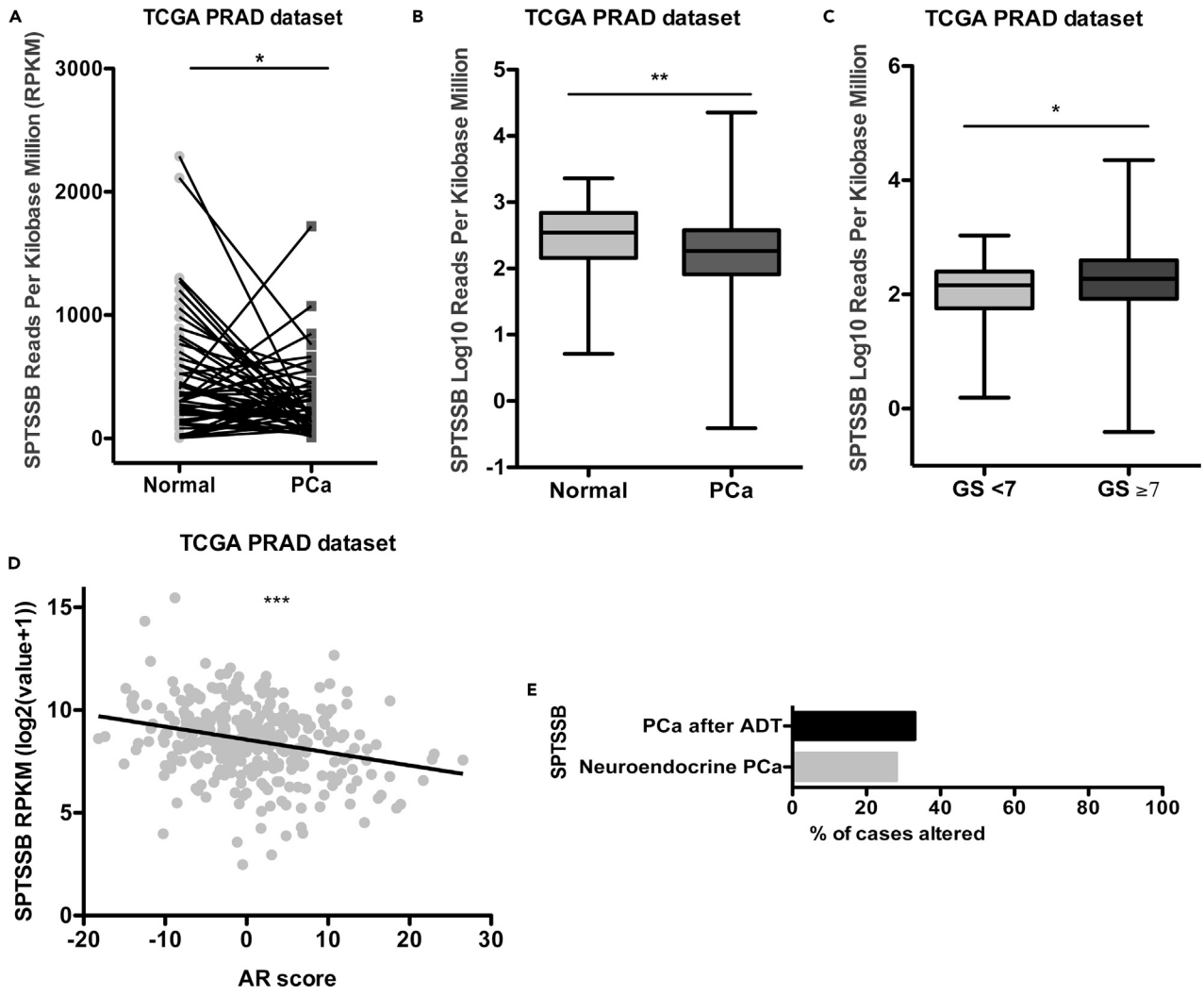

Figure 5. SPTSSB Expression Is Elevated in Patients with Neuroendocrine PCa

(A) SPTSSB expression from matched normal and tumor samples available in PRAD TCGA data set (n = 52). *p* values obtained using non-parametric Mann–Whitney *U*-test: * represent significance of p values < 0.05.

(B) Log10 expression of SPTSSB in PRAD TCGA dataset (RNA-seq) in normal samples (n = 52) and patients with PCa (n = 497). *p* values obtained using non-parametric Mann–Whitney *U*-test: ** represent significance of p values < 0.01.

(C) Expression of SPTSSB in PRAD TCGA dataset segregated by Gleason score <7 (n = 45) and ≥7 (n = 452). *p* values obtained using non-parametric Mann–Whitney *U*-test: * represent significance of p values < 0.05.

(D) Correlation between expression of SPTSSB and AR score in PRAD TCGA data set (n = 332). *p* values obtained using Spearman correlation: *** represent significance of p values < 0.001.

(E) SPTSSB is altered in 33% of patients after ADT (27% with upregulation or amplification) (n = 63) (Kumar et al., 2016) and amplified or upregulated in 28% of neuroendocrine PCa samples (n = 81) (Beltran et al., 2016).

ADT (17 of 63 cases) (Figure 5E) (Kumar et al., 2016). These results argue that elevated SPTSSB expression plays a significant role in aggressive, metastatic cases that have been treated with ADT.

SPTSSB Is Necessary for Regulating *De Novo* Synthesis of Ceramide, which Determines CNL Efficacy in AR-Negative Cells

Given the prominent role that *de novo* synthesis plays in the efficacy of CNL in AR-negative cells and the observed elevation of *SPTSSB* in the aggressive ADT-treated PCa tumors, we examined the effect of CNL treatment after knock down of *SPTSSB* in AR-negative PC-3 cells. PC-3 cells transfected with siRNA targeting *SPTSSB* showed a reduction in *SPTSSB* expression as well as visible changes in cell morphology (Figure 6A, data not shown). Interestingly, *SPTSSB* knockdown in PC-3 cells diminished cell viability without

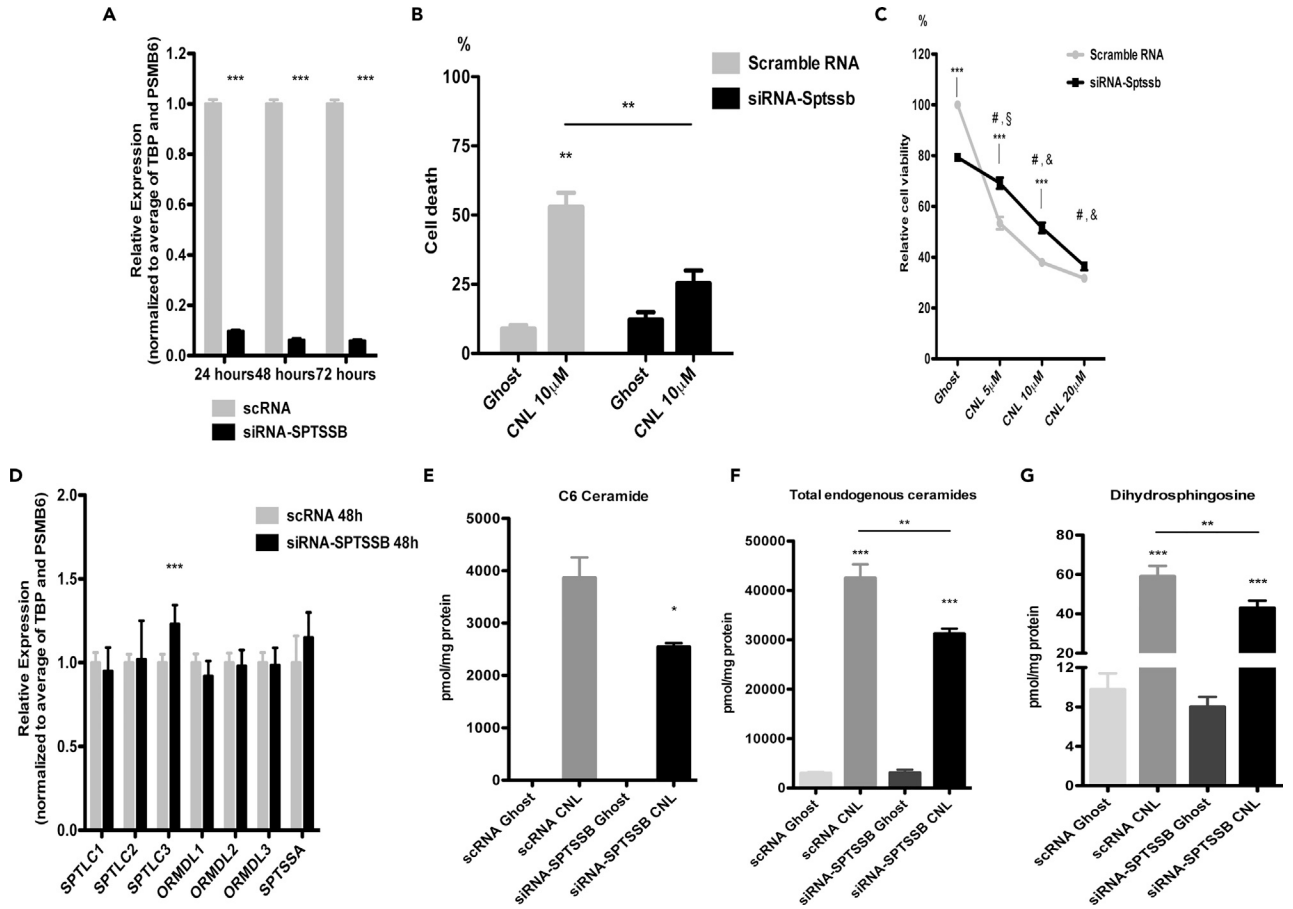

Figure 6. SPTSSB Is Essential for CNL Efficacy in AR-Negative Cells

(A) Expression of SPTSSB after knockdown in PC-3 cells compared to scramble control. Mean ± SEM from three independent experiments is represented. *p* values obtained using non-parametric Mann–Whitney *U*-test: *** represent significance of p values < 0.001.

(B) Cell death of PC-3 cells transfected with scRNA and siRNA-SPTSSB and 24hr later treated with CNL or ghost for 48hr. Mean ± SEM from three independent experiments is represented. *p* values obtained using non-parametric Mann–Whitney *U*-test: ** represent significance of p values < 0.01.

(C) Viability in PC-3 cells transfected with scRNA and siRNA-SPTSSB and 24hr later treated with CNL or ghost for 48hr. Mean ± SEM from three independent experiments is represented. Statistics were obtained using non-parametric Mann–Whitney *U*-test: represented by * in CNL scRNA vs siRNA; § represents p < 0.01 in ghost siRNA vs CNL siRNA; & p < 0.001 in ghost siRNA vs CNL siRNA; #p < 0.001 in ghost scRNA vs CNL scRNA.

(D) Gene expression of SPTLC1-3, ORMDL1-3, SPTSSA in PC-3 cells after knocking down SPTSSB compared to scramble control. Mean ± SEM from three independent experiments is represented. *p* values obtained using non-parametric Mann–Whitney *U*-test: *** represent significance of p values < 0.001.

(E–G) Mass of (E) C6-ceramide, (F) total endogenous ceramides, (G) dihydrosphingosine in PC-3 cells transfected with scRNA and siRNA-SPTSSB for 24hr followed by treatment with ghost or CNL for 24hr (10μM). Mean ± SEM (n = 4) is represented. *p* values obtained using a two-tailed *t* test: *, **, and *** represent significance of p values < 0.05, 0.01, and 0.001, respectively.

increasing cellular death (Figures 6B and 6C). The efficacy of CNL was significantly hindered after *SPTSSB* knockdown as the effect on cell death and viability was reduced in cells treated with siRNA-*SPTSSB* compared to the control siRNA-scramble (Figures 6B and 6C). We confirmed that knockdown of *SPTSSB* was not compensated for by an overall increase in the expression of other enzymes involved in *de novo* synthesis of sphingolipids (Figure 6D). These data show that SPTSSB is necessary for maximum efficacy of CNL in AR-negative cells.

We next sought to determine the importance of SPTSSB in sphingolipid generation. After 24hr of SPTSSB knock down, PC-3 cells were challenged with CNL for 24hr, and sphingolipid masses were measured. We observed that knocking down *SPTSSB* for 48 hr did not change sphingolipid mass in PC-3 cells (Figures 6E–6G). However, upon CNL treatment, the knockdown of *SPTSSB* reduced the levels of C6-ceramide (Figure 6E) and total endogenous ceramides (Figure 6F). Notably, the mass of dihydrosphingosine, indicative of *de novo* synthesis of sphingolipids, was reduced in the siRNA-SPTSSB cells treated with CNL compared

with scramble RNA (Figure 6G). The lower levels of ceramide accumulated in the siRNA-SPTSSB cells after CNL treatment correlates with reduced efficacy of CNL. This shows, for the first time, that SPTSSB-dependent *de novo* synthesis of sphingolipids is critical for maximum CNL efficacy in AR-negative PCa cells.

DISCUSSION

Patients with PCa that relapse to CRPCa currently have no viable therapeutic options and will ultimately die from the disease. In this study, we show that CNLs are an efficacious treatment for CRPCa AR-negative cells that represent the most aggressive stage of the disease. We also show that combining CNLs with FDA-approved drugs against the AR signaling axis results in enhanced effect in the more-common AR-positive cells. Thus, we postulate that the enhanced effect of combining AR signaling inhibitors and CNL in PCa is promising to (1) prevent relapse and neuroendocrine differentiation, and (2) to treat metastatic advanced PCa with neuroendocrine differentiation that currently have no other options. Though rare, AR-positive cells that survive ADT can relapse and transdifferentiate leading to highly aggressive neuroendocrine tumors (Davies et al., 2018; Li et al., 2018; Zou et al., 2017). These tumors have no current therapeutic options, showing potential for CNL in a clinical setting of PCa.

When we assessed metabolism of CNL in the PCa models, we found that CNL induced an accumulation of ceramides driven by an increase of *de novo* synthesis of sphingolipids in both AR-negative cells and in AR-positive cells treated with anti-androgens. Although previous work showed non-liposomal C6 and C2-ceramides to be effective against LNCaP cells (Gewies et al., 2000; Wang et al., 1999), we could not recapitulate this finding with either nanoliposomal C6-ceramide or non-liposomal C6-ceramide (data not shown). To our knowledge, this study is the first to demonstrate that PCa cells respond to CNL depending on their AR status, with AR-positive cells being less responsive.

We evaluated a rate-limiting *de novo* sphingolipid synthesis co-factor SPTSSB, as regulated by AR signaling and its importance in activation of *de novo* synthesis in PCa cells. Not only did blocking androgen signaling lead to increased expression of *SPTSSB* in AR-positive cells, but CNL treatment increased *SPTSSB* expression further. Additionally, *in vitro* and *in silico* analysis of *SPTSSB* expression suggest that this enzyme is upregulated in more aggressive ADT-treated PCa tumors and that *SPTSSB* levels can potentially serve as a biomarker for clinical outcome. Importantly, in a study published by Li e al., CRPCa xenografts of LNCaP cells significantly upregulated SPTSSB, both in response to castration as well as resistance to enzalutamide (Li et al., 2018). These findings identify a possible dysregulation of the *de novo* pathway under AR-negative conditions in PCa and an Achilles' heel that could be exploited by ceramide-centric therapeutics. Of particular interest, our studies document that CNL can target this pathway by driving SPTSSB-dependent generation of dihydrosphingosine that can lead to accumulation of pro-death ceramide species. Notwithstanding, accumulation of dihydrosphingosine caused by an activating mutation in SPTSSB has been shown to lead to neurodegeneration (Zhao et al., 2015).

As for exactly how dysregulation of sphingolipid metabolism may be triggering cell death in response to CNL treatment, researchers have proposed a rheostat model where sphingosine-1-phosphate (S1P) determines cell fate by counterbalancing the death-inducing ceramide (Newton et al., 2015). Recently, we have modified this idea to encompass other sphingolipid metabolic pathways. We postulated that each cell has a pool of ceramide and several escape routes to avoid cell death by ceramide accumulation (Shaw et al., 2018). In AR-negative PCa cells, we suggest that the administration of exogenous ceramides overloads the ceramide pool and also increases *de novo* lipid synthesis leading to cell death. Our data provides an exception to previously reported data that exogenous ceramides shuts down the *de novo* synthesis of sphingolipids, perhaps, to avoid cell death by unnecessary accumulation of ceramides (Siow and Wattenberg, 2012). We postulate that AR-negative cells have unchecked *de novo* synthesis of sphingolipids that can then be further increased by ceramide-based therapeutics leading to cell death. We observed that the increase in dihydrosphingosine after CNL treatment is accompanied by increased transcription of multiple enzymes involved in the *de novo* synthesis of sphingolipids.

Of the enzymes upregulated by ceramide-based therapeutics, serine palmitoyltransferase small subunit B (SPTSSB) is of special importance as it has been shown to maximize the ability of mammalian cells to initiate *de novo* sphingolipid synthesis (Han et al., 2009; Harmon et al., 2013; Singh et al., 2005). This small subunit has been understudied, but its importance is now becoming clearer in multiple different fields (Adachi et al., 2018; Davis et al., 2020; Kojima et al., 2018; Zhao et al., 2015). The first publication regarding SPTSSB

showed that androgens decreased its expression in mice prostate without identifying the function of the protein or implication in disease (Singh et al., 2005). A recent work showed that the maturation of oligodendroctyes and myelination progression occurred concomitantly to increased expression of SPTSSB (Davis et al., 2020). Our data further supports the importance of this small subunit as we report significant differences between AR-positive and AR-negative cells in terms of response to exogenous ceramides and regulation of *de novo* synthesis. One of the more interesting questions arising from our work is how unchecked *de novo* sphingolipid synthesis potentially benefits aggressive PCa cell survival. Speculations around ceramide localization, signaling cascades, and metabolism to less toxic lipid species have all been considered. One potential explanation to this question is the increased synthesis of pro-mitogenic gangliosides in response to ceramide, an observation previously documented (Ravindranath et al., 2004). In fact, our studies do not sufficiently answer this intriguing observation. Despite uncertainty around the oncological benefits of increased/unregulated *de novo* synthesis in AR-negative PCa, our studies identify this pathway as an avenue to be exploited by ceramide-centric therapeutics.

Our study also provides insight into the expression of *SPTSSB* in data sets of patients with PCa. Strikingly, in a neuroendocrine data set, *SPTSSB* was significantly upregulated in almost a quarter of the cases. This supports our hypothesis that SPTSSB expression increases in cells that resist AR signaling inhibition. More molecular studies are necessary to determine at what point in the PCa progression does SPTSSB activity increase and if this enzyme can be used as a predictive biomarker for patients whom can benefit from ceramide-based therapeutics. Importantly, it is necessary to expand the data sets currently made available by scientific consortiums to include lipidomics in order to obtain a more complete picture of tumor pathogenesis. In 2017, studies on two cohorts of patients with PCa showed that of 19 plasma lipid signatures important for prognostic evaluation, 12 were sphingolipid species (gangliosides, ceramides and sphingomyelins) (Lin et al., 2017). This groundbreaking study identifies sphingolipid changes as biomarkers for prognosis, but lacks depth in number of sphingolipid species analyzed. Our results point to a potential role of *de novo* sphingolipid synthesis in the progression of the disease and suggest evaluating sphingolipids involved in this process would improve our understanding of PCa and its development.

Collectively, our data provide rationale for the clinical use of CNL, potentially in combination with AR signaling inhibitors, for patients with PCa before, and after, relapse to CRPCa. More importantly, we show for the first time that in neuroendocrine cells, aberrant *de novo* synthesis of sphingolipids is important for response to ceramide-based therapeutics and is dependent on *SPTSSB*. This subunit was previously described as downregulated by androgens in mice (Singh et al., 2005) and our work now shows that pharmacological impairment of AR signaling increases *SPTSSB* expression and *de novo* synthesis of sphingolipids. This SPTSSB-driven increase in *de novo* synthesis enhances the efficacy of CNL in AR-positive models post-AR signaling inhibition. These findings further our understanding of the role of SPTSSB-dependent *de novo* synthesis of sphingolipids in PCa and offer a molecular mechanism that could be used to improve PCa treatment options.

Limitations of the Study

We have showed that CNL is a promising therapeutic option for all patients with PCa. We postulate that the combination of CNL with already FDA-approved anti-androgens will have enhanced effect against prostate tumors. These results were validated in several *in vitro* models of PCa. However, this important finding needs to be validated in more translationally relevant *in vivo* models of the disease. In addition, the AR-dependent negative regulation of sphingolipid *de novo* synthesis modulated by SPTSSB is a novel molecular pathway that can be explored for improved PCa therapeutics. However, it is still not fully clear how cells respond to exogenous and endogenous ceramides to regulate this putative negative feedback loop. Further research is necessary to define how human cells sense exogenous ceramides.

Resource Availability

Lead Contact

Further information and requests for resources and reagents should be directed to and will be fulfilled by the Lead Contact, Mark Kester (mk5vq@virginia.edu).

Materials Availability

This study did not generate unique reagents.

Data and Code Availability

This study did not generate any unique data sets or code.

METHODS

All methods can be found in the accompanying Transparent Methods supplemental file.

SUPPLEMENTAL INFORMATION

Supplemental Information can be found online at https://doi.org/10.1016/j.isci.2020.101855.

ACKNOWLEDGMENTS

The authors would like to thank Dr. Daniel Gioeli and Dr. Christina Voelkel-Johnson for kindly gifting the experimental models used in this study. The graphical abstract was created using BioRender.com. This work was funded by the Farrow Fellowship from the University of Virginia Cancer Center. Mass spectrometry services were supported by the National Cancer Institute (P30CA44579). P.C-P was funded by the National Cancer Institute of the National Institutes of Health (F99CA245802, P30CA44579). The content is solely the responsibility of the authors and does not necessarily represent the official views of the National Institutes of Health.

AUTHOR CONTRIBUTIONS

Conceptualization: P.C-P., T.E.F., and M.K.; Methodology development: P.C-P, S.J.W., and T.E.F.; Data acquisition: P.C-P., A.H., M.H.R., K.J. and T.E.F.; Formal analysis: P.C-P., K.J., T.E.F.; Writing original draft: P.C-P., T.E.F., and M.K.; Writing - Review & Editing: A.H., M.H.R., J.J.P.S., K.J., and B.P.; Supervision: M.K.

DECLARATION OF INTERESTS

Ceramide Nanoliposomes have been licensed to Keystone Nano Inc. (State College, PA) by the Penn State Research Foundation. M.K. is CMO and co-founder of Keystone Nano Inc. This work has been issued a provisional patent number: PCT/US2018/059259, WO2019/090255.

Received: August 26, 2020
Revised: October 23, 2020
Accepted: November 19, 2020
Published: December 18, 2020

REFERENCES

Adachi, R., Asano, Y., Ogawa, K., Oonishi, M., Tanaka, Y., and Kawamoto, T. (2018). Pharmacological characterization of synthetic serine palmitoyltransferase inhibitors by biochemical and cellular analyses. Biochem. Biophys. Res. Commun. *497*, 1171–1176.

Aggarwal, R., Zhang, T., Small, E.J., and Armstrong, A.J. (2014). Neuroendocrine prostate cancer: subtypes, biology, and clinical outcomes. J. Natl. Compr. Canc. Netw. *12*, 719–726.

Barth, B.M., Cabot, M.C., and Kester, M. (2011). Ceramide-based therapeutics for the treatment of cancer. Anticancer Agents Med. Chem. *11*, 911–919.

Beckham, T.H., Lu, P., Cheng, J.C., Zhao, D., Turner, L.S., Zhang, X., Hoffman, S., Armeson, K.E., Liu, A., Marrison, T., et al. (2012). Acid ceramidase-mediated production of sphingosine 1-phosphate promotes prostate cancer invasion through upregulation of cathepsin B. Int. J. Cancer *131*, 2034–2043.

Beltran, H., Prandi, D., Mosquera, J.M., Benelli, M., Puca, L., Cyrta, J., Marotz, C., Giannopoulou, E., Chakravarthi, B.V., Varambally, S., et al. (2016). Divergent clonal evolution of castration-resistant neuroendocrine prostate cancer. Nat. Med. *22*, 298–305.

Cerami, E., Gao, J., Dogrusoz, U., Gross, B.E., Sumer, S.O., Aksoy, B.A., Jacobsen, A., Byrne, C.J., Heuer, M.L., Larsson, E., et al. (2012). The cBio cancer genomics portal: an open platform for exploring multidimensional cancer genomics data. Cancer Discov. *2*, 401–404.

Damber, J.E., and Aus, G. (2008). Prostate cancer. Lancet *371*, 1710–1721.

Davies, A.H., Beltran, H., and Zoubeidi, A. (2018). Cellular plasticity and the neuroendocrine phenotype in prostate cancer. Nat. Rev. Urol. *15*, 271–286.

Davis, D., Kannan, M., and Wattenberg, B. (2018). Orm/ORMDL proteins: gate guardians and master regulators. Adv. Biol. Regul. *70*, 3–18.

Davis, D.L., Mahawar, U., Pope, V.S., Allegood, J., Sato-Bigbee, C., and Wattenberg, B.W. (2020). Dynamics of sphingolipids and the serine-palmitoyltransferase complex in rat oligodendrocytes during myelination. J. Lipid Res. *61*, 505–522.

de Launoit, Y., Veilleux, R., Dufour, M., Simard, J., and Labrie, F. (1991). Characteristics of the biphasic action of androgens and of the potent antiproliferative effects of the new pure antiestrogen EM-139 on cell cycle kinetic parameters in LNCaP human prostatic cancer cells. Cancer Res. *51*, 5165–5170.

Di Pardo, A., Basit, A., Armirotti, A., Amico, E., Castaldo, S., Pepe, G., Marracino, F., Buttari, F., Digilio, A.F., and Maglione, V. (2017). De novo synthesis of sphingolipids is defective in experimental models of Huntington's disease. Front Neurosci. *11*, 698.

Dolgachev, V., Farooqui, M.S., Kulaeva, O.I., Tainsky, M.A., Nagy, B., Hanada, K., and Separovic, D. (2004). De novo ceramide accumulation due to inhibition of its conversion to complex sphingolipids in apoptotic photosensitized cells. J. Biol. Chem. *279*, 23238–23249.

Felici, A., Pino, M.S., and Carlini, P. (2012). A changing landscape in castration-resistant

prostate cancer treatment. Front. Endocrinol. *3*, 85.

Gewies, A., Rokhlin, O.W., and Cohen, M.B. (2000). Ceramide induces cell death in the human prostatic carcinoma cell lines PC3 and DU145 but does not seem to be involved in Fas-mediated apoptosis. Lab. Invest. *80*, 671–676.

Grosch, S., Schiffmann, S., and Geisslinger, G. (2012). Chain length-specific properties of ceramides. Prog. Lipid Res. *51*, 50–62.

Han, G., Gupta, S.D., Gable, K., Niranjanakumari, S., Moitra, P., Eichler, F., Brown, R.H., Jr., Harmon, J.M., and Dunn, T.M. (2009). Identification of small subunits of mammalian serine palmitoyltransferase that confer distinct acyl-CoA substrate specificities. Proc. Natl. Acad. Sci. U. S. A. *106*, 8186–8191.

Hannun, Y.A., and Obeid, L.M. (2018). Sphingolipids and their metabolism in physiology and disease. Nat. Rev. Mol. Cell Biol. *19*, 175–191.

Harmon, J.M., Bacikova, D., Gable, K., Gupta, S.D., Han, G., Sengupta, N., Somashekarappa, N., and Dunn, T.M. (2013). Topological and functional characterization of the ssSPTs, small activating subunits of serine palmitoyltransferase. J. Biol. Chem. *288*, 10144–10153.

Kester, M., Bassler, J., Fox, T.E., Carter, C.J., Davidson, J.A., and Parette, M.R. (2015). Preclinical development of a C6-ceramide NanoLiposome, a novel sphingolipid therapeutic. Biol. Chem. *396*, 737–747.

Kojima, T., Asano, Y., Kurasawa, O., Hirata, Y., Iwamura, N., Wong, T.T., Saito, B., Tanaka, Y., Arai, R., Yonemori, K., et al. (2018). Discovery of novel serine palmitoyltransferase inhibitors as cancer therapeutic agents. Bioorg. Med. Chem. *26*, 2452–2465.

Kolesnick, R., and Fuks, Z. (2003). Radiation and ceramide-induced apoptosis. Oncogene *22*, 5897–5906.

Kumar, A., Coleman, I., Morrissey, C., Zhang, X., True, L.D., Gulati, R., Etzioni, R., Bolouri, H., Montgomery, B., White, T., et al. (2016). Substantial interindividual and limited intraindividual genomic diversity among tumors from men with metastatic prostate cancer. Nat. Med. *22*, 369–378.

Lee, C., Sutkowski, D.M., Sensibar, J.A., Zelner, D., Kim, I., Amsel, I., Shaw, N., Prins, G.S., and Kozlowski, J.M. (1995). Regulation of proliferation and production of prostate-specific antigen in androgen-sensitive prostatic cancer cells, LNCaP, by dihydrotestosterone. Endocrinology *136*, 796–803.

Li, Q., Deng, Q., Chao, H.-P., Liu, X., Lu, Y., Lin, K., Liu, B., Tang, G.W., Zhang, D., and Tracz, A. (2018). Linking prostate cancer cell AR heterogeneity to distinct castration and enzalutamide responses. Nat. Commun. *9*, 1–17.

Lin, H.M., Mahon, K.L., Weir, J.M., Mundra, P.A., Spielman, C., Briscoe, K., Gurney, H., Mallesara, G., Marx, G., Stockler, M.R., et al. (2017). A distinct plasma lipid signature associated with poor prognosis in castration-resistant prostate cancer. Int. J. Cancer *141*, 2112–2120.

Maceyka, M., and Spiegel, S. (2014). Sphingolipid metabolites in inflammatory disease. Nature *510*, 58–67.

McNair, C., Urbanucci, A., Comstock, C.E., Augello, M.A., Goodwin, J.F., Launchbury, R., Zhao, S.G., Schiewer, M.J., Ertel, A., Karnes, J., et al. (2017). Cell cycle-coupled expansion of AR activity promotes cancer progression. Oncogene *36*, 1655–1668.

Mills, I.G. (2014). Maintaining and reprogramming genomic androgen receptor activity in prostate cancer. Nat. Rev. Cancer *14*, 187–198.

Modrak, D.E., Gold, D.V., and Goldenberg, D.M. (2006). Sphingolipid targets in cancer therapy. Mol. Cancer Ther. *5*, 200–208.

Murdica, V., Mancini, G., Loberto, N., Bassi, R., Giussani, P., Di Muzio, N., Deantoni, C., Prinetti, A., Aureli, M., and Sonnino, S. (2018). Abiraterone and ionizing radiation alter the sphingolipid homeostasis in prostate cancer cells. Adv. Exp. Med. Biol. *1112*, 293–307.

Nadiminty, N., Tummala, R., Liu, C., Yang, J., Lou, W., Evans, C.P., and Gao, A.C. (2013). NF-kappaB2/p52 induces resistance to enzalutamide in prostate cancer: role of androgen receptor and its variants. Mol. Cancer Ther. *12*, 1629–1637.

Narayanan, S., Srinivas, S., and Feldman, D. (2016). Androgen-glucocorticoid interactions in the era of novel prostate cancer therapy. Nat. Rev. Urol. *13*, 47–60.

Newton, J., Lima, S., Maceyka, M., and Spiegel, S. (2015). Revisiting the sphingolipid rheostat: Evolving concepts in cancer therapy. Exp. Cell Res. *333*, 195–200.

Ogretmen, B. (2018). Sphingolipid metabolism in cancer signalling and therapy. Nat. Rev. Cancer *18*, 33–50.

Ramon, J., and Denis, L. (2007). Prostate Cancer (Springer).

Ravindranath, M.H., Muthugounder, S., Presser, N., Selvan, S.R., Portoukalian, J., Brosman, S., and Morton, D.L. (2004). Gangliosides of organ-confined versus metastatic androgen-receptor-negative prostate cancer. Biochem. Biophys. Res. Commun. *324*, 154–165.

Richards, J., Lim, A.C., Hay, C.W., Taylor, A.E., Wingate, A., Nowakowska, K., Pezaro, C., Carreira, S., Goodall, J., Arlt, W., et al. (2012). Interactions of abiraterone, eplerenone, and prednisolone with wild-type and mutant androgen receptor: a rationale for increasing abiraterone exposure or combining with MDV3100. Cancer Res. *72*, 2176–2182.

Ryland, L.K., Fox, T.E., Liu, X., Loughran, T.P., and Kester, M. (2011). Dysregulation of sphingolipid metabolism in cancer. Cancer Biol. Ther. *11*, 138–149.

Saad, A.F., Meacham, W.D., Bai, A., Anelli, V., Elojeimy, S., Mahdy, A.E., Turner, L.S., Cheng, J., Bielawska, A., Bielawski, J., et al. (2007). The functional effects of acid ceramidase overexpression in prostate cancer progression and resistance to chemotherapy. Cancer Biol. Ther. *6*, 1455–1460.

Shaw, J., Costa-Pinheiro, P., Patterson, L., Drews, K., Spiegel, S., and Kester, M. (2018). Novel sphingolipid-based cancer therapeutics in the personalized medicine era. Adv. Cancer Res. *140*, 327–366.

Shen, M.M., and Abate-Shen, C. (2010). Molecular genetics of prostate cancer: new prospects for old challenges. Genes Dev. *24*, 1967–2000.

Siegel, R.L., Miller, K.D., and Jemal, A. (2020). Cancer statistics, 2020. CA Cancer J. Clin. *70*, 7–30.

Singh, J., Young, L., Handelsman, D.J., and Dong, Q. (2005). Molecular cloning and characterization of a novel androgen repressible gene expressed in the prostate epithelium. Gene *348*, 55–63.

Siow, D.L., and Wattenberg, B.W. (2012). Mammalian ORMDL proteins mediate the feedback response in ceramide biosynthesis. J. Biol. Chem. *287*, 40198–40204.

Taha, T.A., Mullen, T.D., and Obeid, L.M. (2006). A house divided: ceramide, sphingosine, and sphingosine-1-phosphate in programmed cell death. Biochim. Biophys. Acta *1758*, 2027–2036.

Tsihlias, J., Zhang, W., Bhattacharya, N., Flanagan, M., Klotz, L., and Slingerland, J. (2000). Involvement of p27Kip1 in G1 arrest by high dose 5 alpha-dihydrotestosterone in LNCaP human prostate cancer cells. Oncogene *19*, 670–679.

Voelkel-Johnson, C., Norris, J.S., and White-Gilbertson, S. (2018). Interdiction of sphingolipid metabolism revisited: focus on prostate cancer. Adv. Cancer Res. *140*, 265–293.

Wang, X.Z., Beebe, J.R., Pwiti, L., Bielawska, A., and Smyth, M.J. (1999). Aberrant sphingolipid signaling is involved in the resistance of prostate cancer cell lines to chemotherapy. Cancer Res. *59*, 5842–5848.

Zhao, L., Spassieva, S., Gable, K., Gupta, S.D., Shi, L.Y., Wang, J., Bielawski, J., Hicks, W.L., Krebs, M.P., Naggert, J., et al. (2015). Elevation of 20-carbon long chain bases due to a mutation in serine palmitoyltransferase small subunit b results in neurodegeneration. Proc. Natl. Acad. Sci. U. S. A. *112*, 12962–12967.

Zong, Y., and Goldstein, A.S. (2013). Adaptation or selection–mechanisms of castration-resistant prostate cancer. Nat. Rev. Urol. *10*, 90–98.

Zou, M., Toivanen, R., Mitrofanova, A., Floch, N., Hayati, S., Sun, Y., Le Magnen, C., Chester, D., Mostaghel, E.A., Califano, A., et al. (2017). Transdifferentiation as a mechanism of treatment resistance in a mouse model of castration-resistant prostate cancer. Cancer Discov. *7*, 736–749.

iScience, Volume *23*

Supplemental Information

Role of SPTSSB-Regulated de Novo Sphingolipid Synthesis in Prostate Cancer Depends on Androgen Receptor Signaling

Pedro Costa-Pinheiro, Abigail Heher, Michael H. Raymond, Kasey Jividen, Jeremy JP. Shaw, Bryce M. Paschal, Susan J. Walker, Todd E. Fox, and Mark Kester

Key Resources Table

REAGENT or RESOURCE	SOURCE	IDENTIFIER
Chemicals, Peptides, and Recombinant Proteins		
CellTiter 96 AQueous MTS Reagent Powder	Promega, Madison, WI	Cat #G1111
Phenazine methosulfate (PMS)	MilliporeSigma, Burlington, MA	Cat #P9625-1G
eBioscience™ Fixable Viability Dye eFluor™ 780	Thermo Fisher Scientific, Waltham, MA	Cat #65-0865-18
L-Serine-13C3	Toronto Research Chemicals, North York, ON, Canada	Cat #S270999
Glutamax	Thermo Fisher Scientific	Cat #35050061
D-erythro-C6-ceramide nanoliposomes	KeystoneNano, State College, PA	N/A
Ghost nanoliposomes	KeystoneNano, State College, PA	N/A
Abiraterone acetate	Selleckchem, Houston, TX	Cat #S2246
Enzalutamide (MDV3100)	Selleckchem	Cat #S1250
5α-Dihydrotestosterone (DHT)	MilliporeSigma	Cat #D-073-1ML
Lipofectamine 2000	Thermo Fisher Scientific	Cat #11668019
Opti-MEM™ I Reduced Serum Medium	Thermo Fisher Scientific	Cat #31985062
RPMI-1640	Thermo Fisher Scientific	Cat #11875-093
DMEM	Thermo Fisher Scientific	Cat #11965-092
DMEM/F12	Thermo Fisher Scientific	Cat #11330033
RPMI 1640 Medium w/o L-Glutamine, L-Serine, HEPES	US Biological,Salem, MA	Cat #R8999-15
Charcoal:Dextran Stripped Fetal Bovine Serum	Gemini Bio Products, West Sacramento, CA	Cat #100-119
Antibiotic Antimycotic (AA)	Thermo Fisher Scientific	Cat #15240062
Insulin-Transferrin-Selenium (ITS)	Corning, Corning, NY	Cat #25-800-CR
Fetal Bovine Serum	Gemini Bio Products	Cat #100-106

Keratinocyte-Serum-Free Media	Thermo Fisher Scientific	Cat #17005042
TRIzol	Thermo Fisher Scientific	Cat #15596018
TrypLE Select	Thermo Fisher Scientific	Cat #12563011
SYTOX™ Green Nucleic Acid Stain	Thermo Fisher Scientific	Cat # S7020
Critical Commercial Assays		
iScript cDNA Synthesis Kit	Bio-Rad, Hercules, CA	Cat #1708891
iTaq Universal Probes Supermix	Bio-Rad	Cat #1725134
Human Cytochrome c Quantikine ELISA Kit	R&D Systems, Minneapolis, MN	Cat #DCTC0
CyQUANT™ NF Cell Proliferation Assay	Thermo Fisher Scientific	Cat #C35006
LDH-Cytotoxicity Assay Kit	Abcam, Cambridge, UK	Cat #ab65393
DC Protein assay	Bio-Rad	Cat #5000112
Deposited Data		
RNA-seq data	(Jividen et al., 2018)	GSE120660
Experimental Models: Cell Lines		
PC-3	Gioeli Lab at the University of Virginia	
LNCaP	Gioeli Lab at the University of Virginia	
DU145	Gioeli Lab at the University of Virginia	
VCaP	Gioeli Lab at the University of Virginia	
C4-2	Gioeli Lab at the University of Virginia	
22Rv1	Gioeli Lab at the University of Virginia	
PC-3/AR+	Paschal Lab at the University of Virginia	(Jividen et al., 2018)
RWPE-1	Paschal Lab at the University of Virginia	

PPC-1	Voelkel-Johnson Lab at Medical University of South Carolina	
Oligonucleotides		
Silencer Select Negative Control No. 1 siRNA	Thermo Fisher Scientific	Cat #4390843
Silencer Select siRNA SPTSSB	Thermo Fisher Scientific	siRNA ID: s46587
PrimePCR FAM probe SPTSSA	Bio-Rad	qHsaCIP0029969
PrimePCR FAM probe SPTSSB	Bio-Rad	qHsaCEP0055358
PrimePCR FAM probe PSMB6	Bio-Rad	qHsaCEP0052321
PrimePCR FAM probe TBP	Bio-Rad	qHsaCIP0036255
PrimePCR FAM probe SPTLC1	Bio-Rad	qHsaCIP0039076
PrimePCR FAM probe SPTLC2	Bio-Rad	qHsaCIP0026692
PrimePCR FAM probe SPTLC3	Bio-Rad	qHsaCEP0054152
PrimePCR FAM probe KLK3	Bio-Rad	qHsaCEP0024737
PrimePCR FAM probe FKBP5	Bio-Rad	qHsaCIP0027271
PrimePCR FAM probe AR	Bio-Rad	qHsaCIP0026366
PrimePCR FAM probe ORMDL1	Bio-Rad	qHsaCEP0051492
PrimePCR FAM probe ORMDL2	Bio-Rad	qHsaCIP0027972
PrimePCR FAM probe ORMDL3	Bio-Rad	qHsaCEP0054129
Software and Algorithms		
GraphPad v5.0 for Mac	GraphPad Software Inc., La Jolla, CA, USA	https://www.graphpad.com/scientific-software/prism/
MassLynx Mass Spectrometry Software v4.1	Waters, Milford, MA	https://www.waters.com/waters/en_US/MassLynx-Mass-Spectrometry-Software

TargetLynx™ Application Manager v4.1	Waters	https://www.waters.com/waters/en_US/TargetLynx-/nav.htm?cid=513791&locale=en_PT
R studio	R Foundation	https://www.r-project.org/
Cytation 3 Gen5 2.09	BioTek, Winooski, VT	https://www.biotek.com/products/software-robotics-software/gen5-microplate-reader-and-imager-software/
CFX Manager 3.1	Bio-Rad, Hercules, CA	https://www.bio-rad.com/en-pt/sku/1845000-cfx-manager-software?ID=1845000
Attune NxT Flow Cytometer Software	Thermo Fisher Scientific	https://www.thermofisher.com/us/en/home/life-science/cell-analysis/flow-cytometry/flow-cytometers/attune-acoustic-focusing-flow-cytometer/attune-cytometer-software.html
Axio Imager.Z1	Zeiss, Oberkochen, Germany	https://www.zeiss.com/microscopy/int/products/imaging-systems/axioscan-z1.html
FlowJo v.10	BD Biosciences, San Jose, CA	https://www.flowjo.com/

Transparent methods

Cell culture

LNCaP and C4–2 cells were grown in DMEM:F12 with 5% Fetal bovine serum, 1% Insulin-Transferrin-Selenium and 1% Antibiotic-Antimicotic (AA). CWR22Rv1 (22Rv1), VCaP, PC-3 were grown in DMEM with 5% Heat-Inactivated serum and 1% AA. DU145 were grown in RPMI-1640 with 10% Heat-Inactivated serum. PC-3/AR+ were grown in RPMI-1640 with 5% Fetal bovine serum and 1% AA. Serum starvation in PC-3/AR+ was accomplished by switching from complete media to RPMI-1640 with 5% of Charcoal stripped FBS and 1% AA. RWPE-1 cells were grown in Keratinocyte-Serum-Free Media. Cells were maintained at 37°C and 5% CO^2 in a humidified chamber.

Cell viability assay

Cells were plated for 24 hours in 96-well plates before treatments. Cell viability was assessed by MTS assay according to manufacturer's instructions. Plates were incubated for 2 hours at 37ºC and absorbance (490nm) was measured after 2 hours using a Cytation 3. Data was normalized to vehicle controls as described in figure legends.

Cell death flow cytometry assay

Cells were plated for 24 hours in 6-well plates and then treated. Cells were ressuspended in Fixable Viability Dye 780 according to the manufacturers' instructions. The Attune Nxt Flow Cytometer was used to collect the data. Forward and side scatter measurements were used to gate for single cells and excluding cell debris. Control cells were incubated at 70ºC for 10 minutes for dead-cell gating. Single-stain compensation controls for viable and dead cells were collected Data were analyzed using FlowJo v.10 software.

Cell death imaging assay

Cells were plated for 24 hours followed by treatment with CNL and ghost for 22 hours. SYTOX™ Green Nucleic Acid Stain was then added to the cells according to manufacturer's instructions. Cells were then imaged using 20x magnification on an Axio Imager.Z1 for a total of 2 hours.

Quantitative reverse transcription PCR

Total RNA was obtained using TRIzol® reagent following the manufacturer's recommendations. RNA concentration and purity of samples were determined on a Cytation 3 plate reader. For the iScript cDNA Synthesis Kit 1μg of RNA was used. PrimePCR FAM probes used in this study are described in the Star methods section. Gene expression was quantified using iTaq Universal Probes Supermix according to manufacturer's instructions, and measured using CFX Connect Real-Time PCR Connection System. Data was analyzed using the comparative Ct method (Schmittgen and Livak, 2008) with the average of PSMB6 and TBP as housekeeping control.

Cytochrome C ELISA

Cells were seeded in 6-well plates and 24h later treated. Cells were collected and lysed following the Human Cytochrome c Quantikine ELISA Kit manufacturer's instructions. After lysis and centrifugation, pellets were further incubated with 0.5% Triton-X100 for 10 minutes at 4ºC followed by centrifugation to obtain the mitochondria fraction. Protein levels from this fraction were then measured using the DC Protein assay and 1μg of protein was used. Cytochrome C levels were then

assessed using the Human Cytochrome c Quantikine ELISA Kit with absorbance was measured at 450nm with wavelength correction at 540nm using a Cytation 3 plate reader.

Cell proliferation

Cells were seeded in 96-well plates and 24 hours later treated. Cell proliferation was then measured using CyQUANT™ NF Cell Proliferation Assay according to manufacturer's instructions. Fluorescence excitation was measured at 485nm and emission at 530nm using a Cytation 3 plate reader.

Cytotoxicity LDH assay

Cells were seeded in 96-well plates and 24 hours later treated. Release of lactate dehydrogenase (LDH) was measured using the LDH-Cytotoxicity Assay Kit according to manufacturer's instructions. Briefly, media was harvested from wells and incubated with LDH Reaction mix. Cell culture media was used as background control and lysed cells respective to each treatment as High control to account for cell number difference. The absorbance was measured at 450 nm on a Cytation 3 plate reader.

Mass spectrometry protocol

Lipid extraction and analysis was done using liquid chromatography-electrospray ionization-tandem mass spectrometry (LC-ESI-MS/MS). Cells were plated in 6-well plates and treated 24h after seeding. Lipids extraction was performed as previously reported (Tan, 2016). All data reported are based on monoisotopic mass and are represented as pmol/mg of protein extracted.

Isotope labeled serine tracing

Serine tracing was performed using isotope labeled L-Serine-13C3 (Toronto Research Chemicals, North York, ON, Canada). Cells were plated in complete media as described above in this section. After allowing cells to adhere for 24 hours, media was replaced with RPMI-1640 w/o L-Glutamine, L-Serine, HEPES with supplemented Glutamax and L-Serine-13C3 at the same concentration as complete RPMI-1640. Fetal bovine serum (10%) and AA (1%) were also added to this media. Cells were kept at 37ºC and 5% CO_2 for 2 hours in this isotope labeled serine media, before being switched to their normal growth media; cells were then treated. Serine tracing was then done following the same mass spectrometry protocol described above.

C6-ceramide Nanoliposome

D-erythro-C6-ceramide nanoliposomes were obtained from KeystoneNano and manufactured according to previous literature (Kester, 2015). The vehicle control nanoliposomes (ghost) was formulated with the same lipid composition except for D-erythro-C6-ceramide. In this study, ghost control was used at a final concentration of 20μM in all experiments.

RNA-sequencing

RNA-sequencing experiment in PCa cells treated with R1881 for 24h and control samples, as well as respective analysis methods are described elsewhere (Jividen et al., 2018).

Knockdown of SPTSSB

Cells were plated and incubated at 37ºC and 5% CO_2 for 16 hours. After 16 hours media was changed to DMEM without FBS and AA for 2 hours. Then, Lipofectamine 2000 was incubated with Opti-Mem according to manufacturer's instructions and added to cells. Silencer Select Negative Control No. 1 siRNA and Silencer Select SPTSSB siRNA-SPTSSB were used for cell transfection at a final concentration of 40nM. For drug treatments, cells were treated 24h after transfection for a total of 72 hours with mRNA levels evaluated every 24 hours according to the protocol above described for knockdown validation.

Prostate cancer patients' gene expression

Data available through the Cancer Genome Atlas (TCGA) (https://www.cancer.gov/tcga) for Prostate cancer (PRAD) dataset was accessed using the TCGA2STAT package using R software. Neuroendocrine datasets was accessed using cBioPortal for differences in expression of SPTSSB in patients (Beltran et al., 2016; Cerami et al., 2012; Kumar et al., 2016). Z-score cutoff used was ± 1.5.

Statistical analysis

Comparisons between two groups were performed using non-parametric Mann–Whitney *U*-test. A two-tailed *t*-test was used to assess differences for cytochrome C ELISA and mass spectrometry experiment following knockdown of *SPTSSB*. *P* values were considered statistically significant if lower than 0.05. All experiments were repeated with a minimum of three independent experiments. Mean and standard error of the mean (SEM) is shown in all figures unless stated. Markers *, **, and *** represent significance of p-values < 0.05, 0.01, and 0.001 respectively. Statistical analysis was performed using GraphPad Prism 5.0 software for Mac (GraphPad Software Inc., La Jolla, CA, USA).

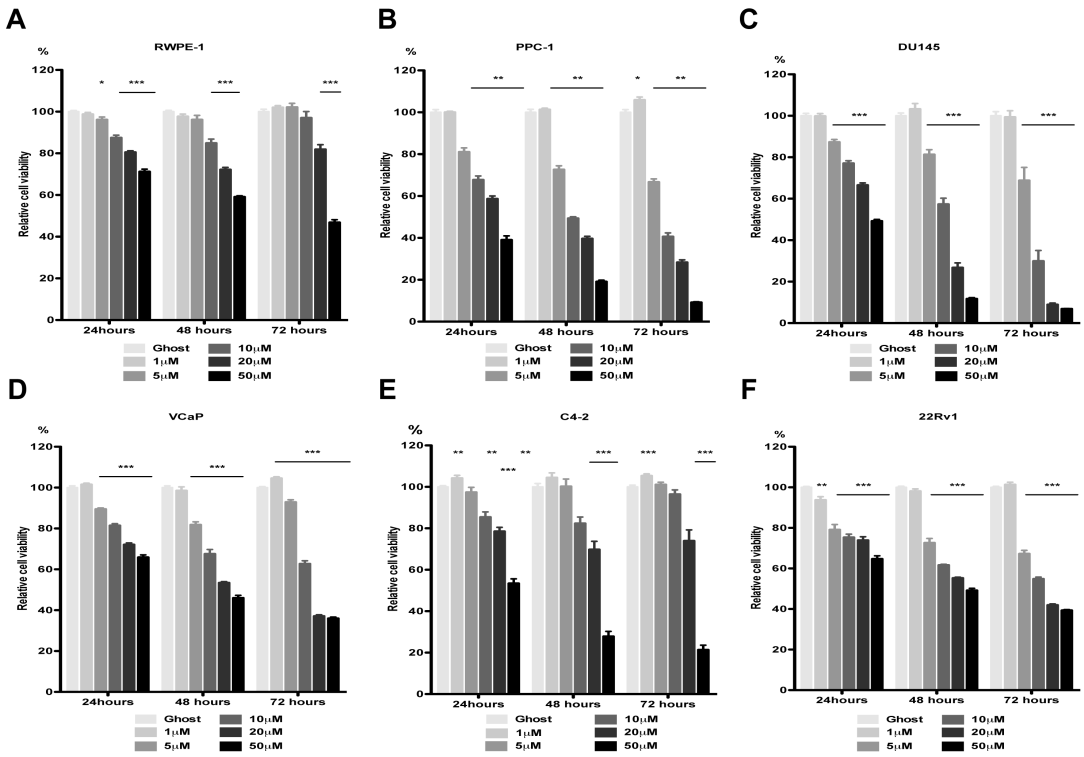

Supplementary Figure 1 – Efficacy of CNL is higher in highly aggressive AR-negative cells, related to Figure 1.

(A-F) Time and concentration effect of CNL on the viability of AR-positive normal prostate cell line (A) RWPE-1; AR-negative PCa cell lines (B) PPC-1, (C) DU145; AR-positive PCa cell lines (D) 22Rv1, (E) VCaP, (F) C4-2, compared to ghost control. Mean ± SEM from three independent experiments is represented. *P* values obtained using non-parametric Mann–Whitney *U*-test: *, **, and *** represent significance of p-values < 0.05, 0.01, and 0.001 respectively.

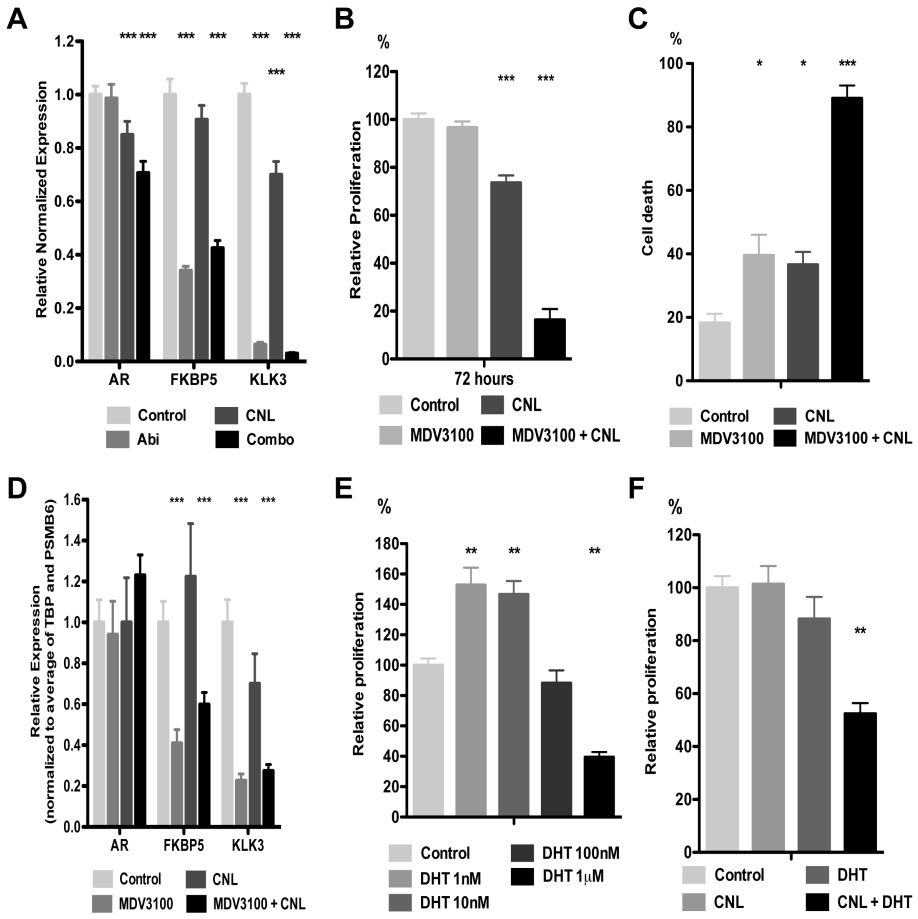

Supplementary Figure 2 – Intact AR signaling hinders CNL efficacy in PCa cells, related to Figure 2.

(A) Gene expression of AR signaling targets in LNCaP cells treated with Abi (10μM), CNL (10μM), or Combo (10μM+10μM) for 48h compared to Negative control (EtOH+ghost). Mean ± SEM from three independent experiments is represented. *P* values obtained using non-parametric Mann–Whitney *U*-test: *** represent significance of p-values < 0.001.

(B) Proliferation of LNCaP cells after 72h of treatment with MDV3100 (30μM), CNL (20μM), or Combo (30μM+20μM) compared to Negative control (DMSO+ghost). Mean ± SEM from three independent experiments is represented. *P* values obtained using non-parametric Mann–Whitney *U*-test: *** represent significance of p-values < 0.001.

(C) Cell death of LNCaP cells after 72h of treatment with Negative control (DMSO+ghost), Abi (20μM), CNL (20μM), or Combo (30μM+20μM) compared to. Mean ± SEM from three independent experiments is represented. *P* values obtained using non-parametric Mann–Whitney *U*-test: * and *** represent significance of p-values < 0.05 and 0.001 respectively.

(D) Gene expression of AR signaling in LNCaP cells treated with MDV3100 (10μM), CNL (10μM), or Combo (10μM+10μM) for 48h compared to Negative control (DMSO+ghost). Mean ± SEM from three independent experiments is represented. *P* values obtained using non-parametric Mann–Whitney *U*-test: *** represent significance of p-values < 0.001.

(E) Proliferation of LNCaP cells treated with Dihydrotestosterone for 72h and compared to Negative control. Mean ± SEM from three independent experiments is

represented. *P* values obtained using non-parametric Mann–Whitney *U*-test: ** represent significance of p-values < 0.01.
(F) Proliferation of LNCaP cells treated with Dihydrotestosterone (100nM) for 24h followed by CNL (10μM) or ghost for 48h and compared to Negative controls. Mean ± SEM from three independent experiments is represented. *P* values obtained using non-parametric Mann–Whitney *U*-test: ** represent significance of p-values < 0.01.